



Automated assessment of bridge guardrails for regional prioritization based on open-source data and deep learning algorithms

Giuseppe Santarsiero

Department of Engineering, University of Basilicata, via dell'Ateneo Lucano, 10, Potenza 85100, Italy

ARTICLE INFO

Keywords:

Bridge
Guardrail
Infrastructure management
Automated assessment
Deep learning
Open-source data
Road safety

ABSTRACT

Guardrails installed on road bridges are essential to the safety of vehicles and road users. However, infrastructure managers often lack accurate and up-to-date inventories of the safety barriers on their bridges. Moreover, the limited availability of financial resources, combined with the lack of adequately trained personnel, makes it difficult for these entities to effectively assess the condition of such critical infrastructure, even though, in most cases, it is only necessary to recognize the barrier code compliance, which could be done even by less trained personnel. This paper proposes an integrated methodology to automate the assessment of road guardrails installed on bridges using open-source data and deep learning (DL) algorithms. Besides the use of the consolidated YOLO (You Only Look Once) object detection algorithm to classify the safety barriers to establish whether they match the current standards, the process innovatively involves the extraction of bridge information from OpenStreetMap (OSM) to construct a database of existing bridges. This latter step is integrated with Google Street View API, for the extraction of images of each bridge's safety barriers to be analysed by YOLO. The synergic concatenation of these three steps (OSM, Google Street View, YOLO) into a unique software tool, provides road managers with a cost-effective and efficient tool to remotely survey the guardrails installed on their bridges, permitting to prioritize maintenance and upgrading interventions. The methodology not only facilitates the task of infrastructure monitoring but also helps ensure the safety of road users by timely identifying non-compliant safety barriers. Finally, the developed procedure allowed to identify non-conforming guardrails on a subset of bridges located in a southern Italy region permitting to compute the intervention cost for their replacement.

1. Introduction and motivation

The management and maintenance of bridge infrastructure is a key priority for road safety, as bridges are critical components in road networks, especially due to their exposure to various mechanical and environmental stresses over time [1]. While a relevant part of the research is dedicated to the bridge structural components' assessment (i. e. what is below the road pavement, [2]), little evidence of research can be found about guardrails (aka safety barriers, safety railings or restraint systems) that are devoted to preventing vehicles to fall from bridges, causing frequently fatal consequences (what is above the road) [3]. The degradation of these bridge components is a significant concern [4], as these barriers are designed to prevent vehicles from leaving the roadway and causing fatal accidents in case of a collision or other hazardous events as stated by standards and codes [5]. In fact, over the past ten years, the two main accidents occurred in Italy that cause more than sixty fatalities, could have been mitigated by the presence of up-to-date barriers [6]. Therefore, ensuring the structural integrity and regulatory

compliance of these barriers is essential for the safety of road users [5].

Following recent disasters such as the Morandi bridge collapse [7] new guidelines for bridge management were issued in Italy [8,9]. However, local authorities responsible for maintaining such infrastructure, including municipalities and provinces, often struggle with several challenges. One major issue is the lack of detailed, up-to-date inventories of the bridges under their jurisdiction [10]. In many cases, infrastructure databases are either incomplete or totally absent, leading to gaps in knowledge about the condition and safety features of bridges, preventing the setting up of Bridge Management Systems (BMS) [11]. This is particularly problematic for older bridges, where safety barriers may not meet current regulatory standards [12].

The limitations faced by local road authorities extend beyond data availability. Many of these agencies operate with limited human and financial resources [13], making it difficult to carry out regular inspections and assessments of bridge infrastructure, even for the only code-compliance classification. The personnel responsible for these tasks is often overwhelmed by serval activities and is unable to assess

E-mail address: giuseppe.santarsiero@unibas.it.

<https://doi.org/10.1016/j.rineng.2025.105210>

Received 7 March 2025; Received in revised form 2 May 2025; Accepted 3 May 2025

Available online 4 May 2025

2590-1230/© 2025 The Author. Published by Elsevier B.V. This is an open access article under the CC BY-NC-ND license (<http://creativecommons.org/licenses/by-nc-nd/4.0/>).

bridge barriers. As a result, non-compliant barriers may remain unnoticed for years, while limited resources are misallocated to less critical infrastructure elements.

A further complicating factor is the huge volume of infrastructure that needs to be managed. In many provinces and municipalities, road authorities are responsible for hundreds of kilometers of roads and hundreds of bridges, often with minimal staffing [14]. Out of the total 850,000 km of roads in Italy (Fig. 1), only 4 % are managed by national agencies (state roads) or concessionaries (motorways). Therefore, municipalities and provinces are responsible for 816,000 km of roads, with the consequent amount of safety barriers on bridges and road edges.

Among the estimated 120,000 bridges in Italy [10], about 30,000 are on state roads or motorways and 90,000 are on local roads. Therefore, conducting manual inspections of each bridge is a time-consuming and resource-intensive process, particularly for remote or difficult-to-access structures. This leads to significant delays in identifying and addressing non-compliant safety barriers, creating potential hazards for road users [15]. Lastly, it must be noted that even when lacking guardrails are identified, their replacement often requires strengthening interventions on the supporting members such as the cantilever part of the bridge slab and the edge curb [6], increasing the fund allocation needed.

In response to these challenges, there is a growing need for automated and integrated systems that can streamline the process of assessing the condition of bridge safety barriers [11]. The possibility of automatically detect guardrail types and condition to speed-up the maintenance processes would solve this problem. As an example, in [16] an automated approach was proposed to automatically detect road distresses and attribute a pavement rating to prioritize interventions. In [17,18] procedures were set up to detect safety barriers, not only along bridges, using laser scanner technologies and other image acquisition devices and vision data fusion techniques to merge information collected through different means. More recently Gao et al. [19] proposed the use of Mobile Laser Scanning (MLS) systems to obtain highly dense 3D point clouds that enable the acquisition of accurate traffic facilities and therefore guardrail types and conditions. These methods, however, require highly specialized personnel, the management of large amount of data and are time-consuming since it is requested that a vehicle travels the road to collect the needed information. Moreover, expensive devices for image acquisition are often necessary.

Given the mentioned constraints, this paper presents a comprehensive methodology for constructing a bridge database using OpenStreetMap, integrating visual data from Google Street View, and applying deep learning algorithms to assess the compliance of bridge safety barriers. In particular, the proposed approach is devoted to the barrier classification to assess its compliance with the current road safety standards, without the purpose of replacing the work of specialized engineering personnel able to assess the functionality, integrity and

effectiveness of any roadside installed barrier.

In fact, the system architecture is organized through Visual Basic for Applications routines in order to manage the process flow through a single digital tool, leading only to the barrier classification. The following sections provide a detailed description of each step in the process and discuss the potential benefits and limitations of this approach.

2. Methodology

Current methodologies for guardrail assessment, are based on visual inspections made by professionals travelling to specified bridge locations to acquire guardrail details such as the type, eventual damage, information about their connection with the bridge supporting elements. This requires traffic limitation consisting of at least one lane closure for each bridge side. This manual approach requires a minimum 4-person team out of which, 3 are related to the lane closure and safety signals installation, and one person (an engineer) dedicated to barrier survey. Such a methodological framework is extremely slow since one survey team can inspect maximum three to four bridges per day. The main source of slowness is represented by the need of installation and uninstallation of the safety apparatus for lane closure. Alternatively, the simple passage on the bridge of a vehicle equipped with a high-resolution acquisition device (e.g., LiDAR) could avoid the need for lane closures, thus permitting a higher productivity, even though forcing to collect a large amount of data (point clouds) to be interpreted through labour-intensive desk work. In this way, about 20 bridges [17] per day could be inspected overall.

When maintenance issues are mainly related to guardrail type detection, in order to make a decision on the need to replace possibly outdated barriers, in theory, design documents could provide information on the originally installed guardrails. However, many bridges—especially on local roads—lack updated documentation (the design documents are often not available), and over time barriers may have been replaced, removed, or degraded without proper recordkeeping. Therefore, relying solely on original documents may not reflect the current state of the infrastructure. In this case, even a remotely acquired image could be enough to greatly speed-up the process of more than one order of magnitude. In this sense, the present paper proposes a procedure to reduce the need for both expensive acquisition devices and time-consuming activities, exploiting already existing data that could be used also for remote detections. In fact, by leveraging open-source tools and advanced data analysis techniques, local authorities can improve the efficiency of their infrastructure management processes while reducing reliance on manual inspections [20]. Open-source geographic data platforms, such as OpenStreetMap (OSM), are particularly promising for this purpose, as they offer detailed, accurate, and freely accessible information about bridges and road networks across almost all the world [21].

OSM databases can serve as the foundation for further analysis, enabling road authorities to monitor and manage their bridge assets more effectively [22]. These databases can be further extended by manually integrating information retained by road managers in a way to give more consistency and completeness to data.

The next step in automating the assessment process involves the use of visual data to evaluate the condition of bridge safety barriers. Google Street View provides a valuable source of panoramic images of road networks and surrounding infrastructure, including bridges [23]. By using the geographic coordinates extracted from OSM, images of the safety barriers on each bridge can be automatically retrieved through the Google Street View API [24]. These images can then be analysed to determine whether the barriers meet current safety standards [5]. The fact that Google Street View could introduce limitations, as incomplete or outdated imagery could significantly impact the assessment accuracy, is not a significant concern in most cases. In fact, imagery is available with a yearly cadence, in some cases even more frequently, with images

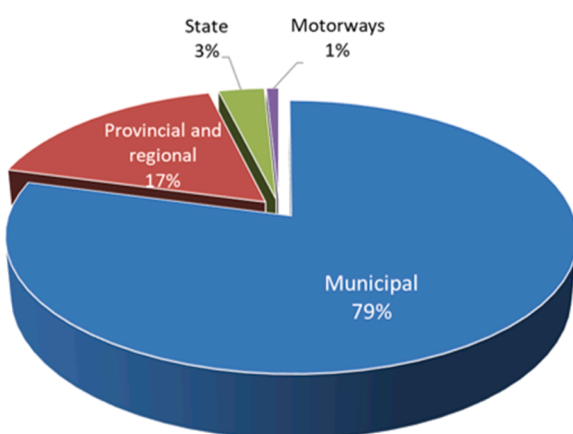


Fig. 1. Shares of roads in Italy by management body.

taken more than once a year (Fig. 2).

Given the volume of data involved, manual analysis of the images is impractical. Instead, deep learning algorithms, such as You Only Look Once (YOLO), can be employed to automate the object detection process. YOLO is an advanced object detection algorithm that has been widely used for infrastructure monitoring and safety assessments [25]. This algorithm has already been successfully used in infrastructure monitoring activities like in [26] in which Yolo was used to detect bridge elastomeric bearing damage, helping in automatically recognizing cracks, shearing and detaching issues in devices.

By training a YOLO model to recognize different types of safety barriers, it is possible to automatically classify the barriers in the Street View images as either compliant or non-compliant with regulatory standards. This automated classification allows local authorities to quickly identify high-risk bridges and prioritize their maintenance efforts, identifying the bridges in need of safety barrier replacement (Fig. 3).

The use of these open-source tools and deep learning techniques (Option 2 in Fig. 3) offers several advantages for local road managers. First, it significantly reduces the time and cost associated with manual inspections (Option 1 in Fig. 3), making it feasible to conduct large-scale assessments of bridge infrastructure [27]. Furthermore, it improves the accuracy and consistency of barrier assessments, minimizing the potential for human error [28]. Finally, it enables local authorities to focus their limited resources on the most critical infrastructure needs, ensuring that non-compliant safety barriers are addressed in a timely manner. It must also be considered that the methodology is mostly automated. Human intervention is required only in two steps such as the initial model training and annotation (done once, the model here presented can be used) and potential manual correction of missing coordinates for bridges in rural areas. In summary, while each individual technology (OSM, GSV, YOLO) is well-established, the novelty of this work lies in their automated integration into a single, low-cost, scalable framework that allows for regional assessment and prioritization of guardrail replacement. This integration is achieved through custom VBA routines that link geospatial data, image retrieval, and deep learning inference in a fully operational tool usable even by non-technical staff. In the following sections, each of the steps involved in the option 2 are described in detail.

2.1. Exploiting open data for bridge dataset development

OpenStreetMap (OSM) is a crowd-sourced geographic database that provides real-time, up-to-date information on various types of infrastructure, including bridges, roads, and pathways. By extracting the geographic coordinates of bridges from OSM, it is possible to construct an infrastructure database that includes critical attributes such as bridge type, location, and connected roadways [21].

To extract bridges from OpenStreetMap, the process begins by defining the geographic area of interest, which can be done using



Fig. 2. Google Street View images available at given timeframes for a specific bridge on a highway.

latitude and longitude coordinates to specify a region. Then, a query is sent to OSM using a tool like the Overpass API to retrieve data tagged as bridges. Bridges in OSM are identified by the tag 'bridge=yes'.

Once the query is executed, the output data typically includes additional information such as the type of road (e.g., motorway, trunk, residential) and other relevant tags, like the structure type or the material of the bridge. This information is extracted and organized into a dataset for further analysis, which can include details such as the bridge's location, length, and associated road network.

The resulting data can be saved in various formats, such as JSON or XML, and further processed for tasks like generating maps or integrating the information into a larger database for infrastructure management. In this case, the database has been treated in Excel environment.

An important piece of information is related to the bridge location. OSM typically provides start and end coordinates, even though, for longer bridges, it also provides a series of intermediate coordinates describing the bridge path. In fact, for bridges longer than approximately 40 m, OSM coordinates every 25 m of length are provided. This allows to estimate the bridge length as well as the heading direction along the bridge development.

One of the main tags in OSM is related to Road type as shown in Table 1 [29]. They have been grouped in major and minor road infrastructures. This is an essential distinction since in minor road infrastructures, safety barriers are often absent due to low traffic volume and the poor pavement installed.

Therefore, the attention will be focused on major road infrastructure, where it is essential guaranteeing the effectiveness of guardrails on bridges.

2.1.1. The Basilicata region bridge dataset

In this study, the proposed methodology was applied to a sample of bridges located in the Basilicata region, Italy. The Basilicata region presents a varied and complex road network, characterized by a combination of national highways, regional roads, and local municipal roads. The bridge dataset for this region includes approximately 2,000 bridges (Fig. 4), which serve as a representative sample for testing the automated barrier assessment methodology described earlier. The construction of this dataset was made possible by exploiting OpenStreetMap (OSM) data and cross-referencing it with official road infrastructure databases.

The dataset contains a variety of information about each bridge, including its geographical location, bridge length, type of road it serves. In the following, it is provided an overview of the distribution of bridges based on their road type and length, highlighting the main characteristics of the dataset.

2.1.2. Bridge distribution by road type

The first factor considered in the analysis is the distribution of bridges according to the type of road they are located on. Fig. 5 shows the distribution of bridge development (in km) across different road types, alongside the percentage of interchanges associated with each road type.

Motorways and trunks (roads that differ from other road types primarily in terms of design, access control, and function within a road network) show a significant portion of bridge development, with approximately 27 to 28 km of bridges respectively. This reflects their importance in supporting heavy traffic volumes and long-distance travel. State Roads exhibit the highest development of bridges, exceeding 60 km in total. This highlights the strategic role these roads play in connecting various towns and cities across Basilicata. Provincial roads follow state roads in terms of bridge length, with roughly 40 km of bridge infrastructure. They serve as essential connectors between smaller municipalities and rural areas. Lastly, municipal roads account for a smaller but still significant portion of bridge development, with about 20 km of length. The remaining bridges are distributed across other road categories, with appreciable lengths observed, summing up

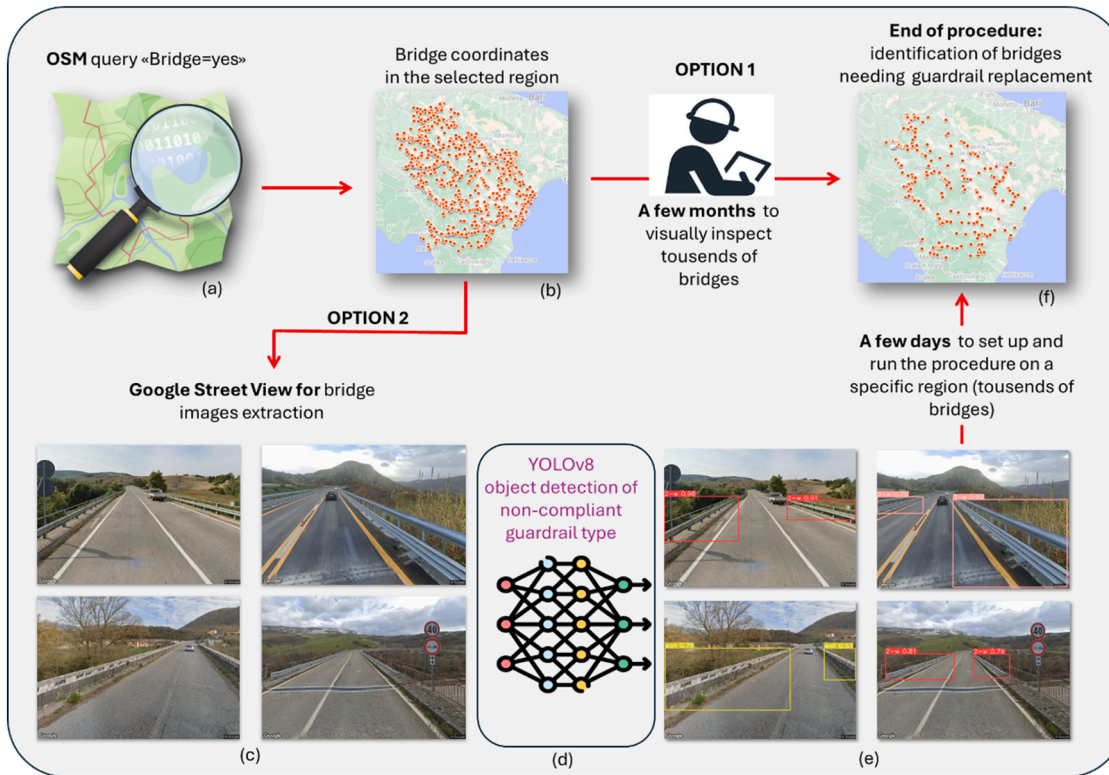


Fig. 3. Framework for remote automated bridge guardrails assessment.

Table 1
Road types classified in OSM datasets.

Group	Road type	Description
Major road infrastructures	motorway	High-speed road, restricted access (e.g., freeways)
	trunk	Major road connecting cities, fewer access controls than motorways
	primary	Main roads linking towns and cities
	secondary	Roads connecting smaller towns and villages
	motorway_link	Short connector roads linking motorways to other roads
	trunk_link	Short connectors linking trunk roads to other roads
	primary_link	Connectors linking primary roads to trunk roads or other roads
	secondary_link	Connectors linking secondary roads to other roads
Minor road infrastructures	tertiary	Roads serving local traffic between smaller settlements
	tertiary_link	Connectors linking tertiary roads to other roads
	unclassified	Minor rural or local roads without a specific classification
	residential	Roads within residential areas, slower speeds
	service	Access roads to services, parking, or industrial areas
	track	Unpaved roads, often used for agriculture or forestry
	pedestrian	Roads or streets designed for pedestrian traffic
	footway	Paths dedicated to pedestrians
	cycleway	Paths dedicated to bicycles
	path	General-purpose paths for non-motorized traffic
	living_street	Low-speed roads prioritizing pedestrians and cyclists
	construction	Roads currently under construction

to >20 km. These are mainly rural roads.

The graph also illustrates the percentage bridges related to interchanges (junctions) for each road type, which is, as expected, highest on highways and progressively decreases on provincial and municipal roads. This is indicative of the higher complexity of the road network and traffic management on major infrastructures compared to smaller roads.

2.1.3. Bridge length distribution

The second factor analysed is the distribution of bridge lengths within the dataset. The bridge length can be calculated using the bridge coordinates, by summing up the length of segments connecting the points that describe the bridge path, from the start to the end point.

Fig. 6 presents the number of bridges categorized by their length and the cumulative percentage of bridges across different length classes. Most bridges (approximately 660 bridges) are relatively short, ranging between 25 and 50 m in length. This is typical for smaller, rural bridges or those crossing minor rivers or streams. Bridges measuring between 10 and 25 m also form a significant portion of the dataset, with 282 bridges falling into this category. Bridges with lengths between 50 and 100 m account for another significant subset, with 320 bridges in this range. As the length increases, the number of bridges decreases. In fact, bridges in the range 100 - 200 m are less common (171 bridges), while longer bridges, such as those spanning 200 to 500 m, number around 103 and 132 respectively. The longest bridges in the dataset, with length between 500 m and 2500 m, are rare, with only a few structures over 1000 m in length.

The cumulative curve shows that 90 % of the bridges in the dataset are <250 m long, while the remaining 10 % are spread across longer length values.

This dataset, composed of bridges from the Basilicata region, serves as a suitable case study for testing the automated system for recognizing and classifying safety barriers. Most bridges are relatively short, yet diverse in their structural characteristics and road types. This diversity enables a thorough evaluation of the proposed methodology across a

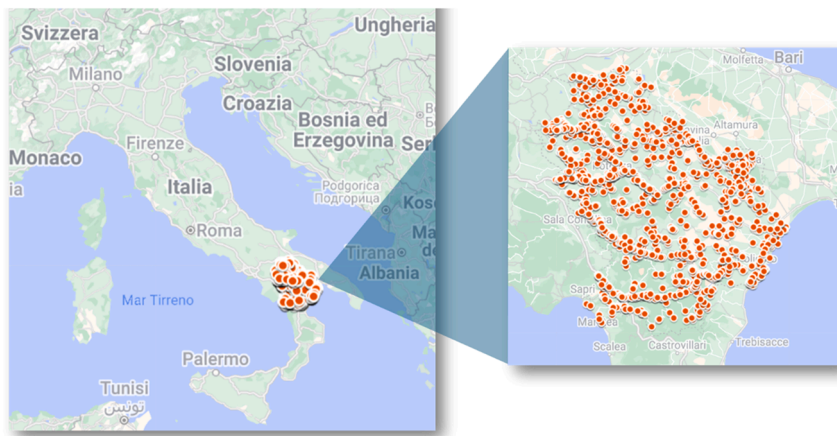


Fig. 4. Geographic locations of bridges included in the dataset.

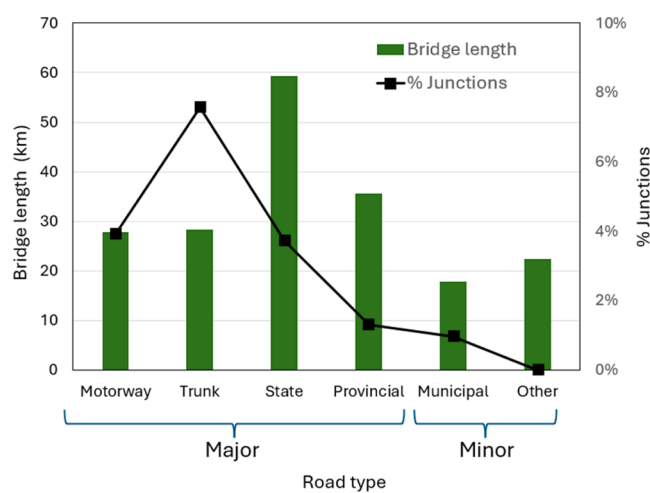


Fig. 5. Distribution of bridge lengths by road type and the percentage of junctions (interchanges).

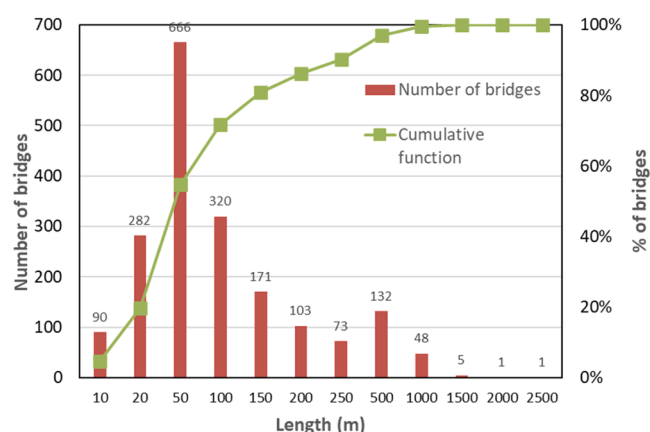


Fig. 6. Length distribution of bridges and viaducts.

wide range of bridge configurations, facilitating the identification of potential non-compliance in safety barrier installations.

2.2. Automated extraction of bridge guardrails images

The process for extracting Street View images of bridges in the

Basilicata region begins with the identification of the geographic coordinates (latitude and longitude) of each bridge, specifically the start and end points. These coordinates are essential for obtaining images that provide a clear view of the road and the guardrails installed on the bridges. The images serve as input for a deep learning system that detects the type of barriers and determines if they comply with current safety regulations.

To capture the images, the Google Street View API is used [24]. This API allows for image retrieval by making an HTTP request that includes parameters such as location, heading, and pitch. The location parameter is provided by the coordinates of the bridge's starting point, while the pitch is fixed at 0 degrees to ensure a horizontal view of the road. This setting is devoted to obtaining a clear, side-on image of the barriers, not an elevated or depressed angle.

The heading parameter, which determines the direction the camera faces, is calculated based on the coordinates of the bridge's start and end points. The heading angle is computed using the following formula, which calculates the angle relative to true North:

$$\theta = \text{atan2}(\sin(LON_2 - LON_1) \cdot \cos(LAT_2), \cos(LAT_1) \cdot \sin(LAT_2) - \sin(LAT_1) \cdot \cos(LAT_2) \cdot \cos(LON_2 - LON_1))$$

Where:

atan2 is a mathematical function that computes the arc tangent of two arguments, y and x , representing the projections on Cartesian plane of the segment connecting points 1 and 2 (assuming that point 1 coincides with the origin, see Fig. 7). Unlike the standard arc tangent function (atan), which only considers the ratio y/x , **atan2** considers both the numerator (y) and denominator (x) to determine the correct angle, considering the quadrant of the point (x, y).

It returns the angle in radians, typically between $-\pi$ and $+\pi$ (or -180° to $+180^\circ$). This makes it especially useful for applications that require precise direction calculations, such as in navigation, robotics, and computer graphics. Thus, **atan2** is a more robust version of the arc tangent function that accurately calculates the angle by considering both coordinates of the point and resolving the quadrant ambiguity (Fig. 7).

- LAT_1, LON_1 are the latitude and longitude of the start point (1),
- LAT_2, LON_2 are the latitude and longitude of the end point (2),
- θ is the resulting heading angle.

Points (1) and (2) are usually the first and the second point provided by OSM as bridge coordinates. As said, for short bridges, they coincide with the start and end points.

The heading angle (θ) ensures that the image is aligned with the direction of the road, providing the optimal view for guardrail detection. The HTTP request to the Google Street View API includes these

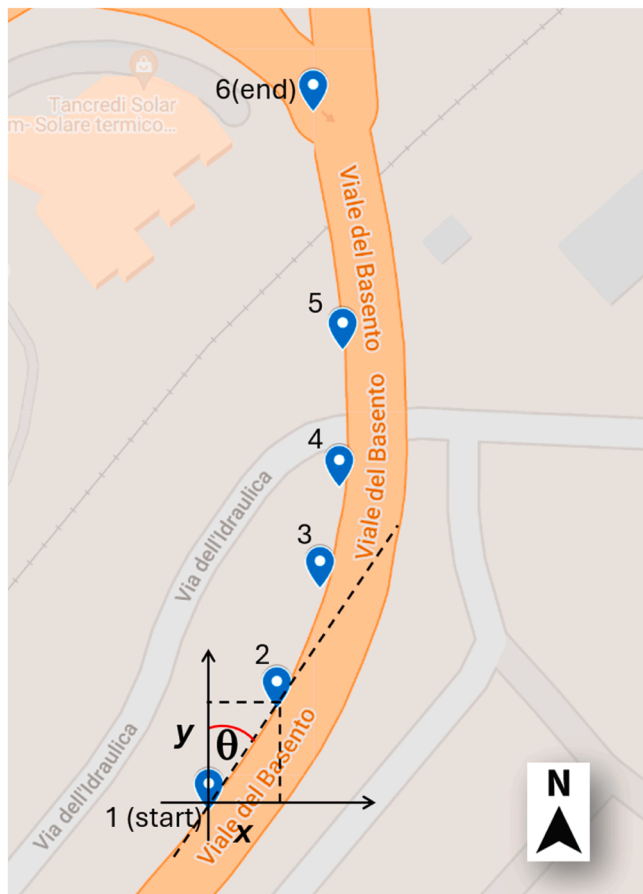


Fig. 7. Example of heading angle calculation (Map adapted from Google MyMaps).

parameters in the following format:

https://maps.googleapis.com/maps/api/streetview?size=640x640&location=LAT, LON&heading=HEADING&pitch=0&key=YOUR_API_KEY
Where:

- LAT, LON are the latitude and longitude coordinates,
- HEADING is the calculated angle θ ,
- pitch=0 ensures a horizontal view,
- key=YOUR_API_KEY is your Google API key (provided upon the activating a Google Cloud account).

In case points (1) and (2) are not aligned along the same road border the calculated heading angle could be not perfectly aligned with the road direction, as can be seen for some of the road pictures in Fig. 8 (e.g., 261, 274 etc....). However, also in these cases the resulting picture can be utilized for the safety barrier recognition and no correction is needed.

The image extraction through the above-mentioned HTTP request is made automatically using a purposely developed Visual Basic for Application [30] subroutine that also saves in a selected folder each image. This routine uses the bridges listed in the database and assigns the bridge ID as picture filename.

The routine was executed for the sample of 1,888 bridges in the Basilicata region on a simple laptop equipped with an Intel(R) Core(TM) provided with 16.0 GB RAM through to a 30 Mbps wireless internet connection. The extraction of all images (640×640 pixel resolution) required 9 min (i.e., 0.286 s/image). Therefore, the procedure is rather efficient, also considering that more powerful computers could be adopted. Out of the 1,888 images, 119 (6.3 %) contain no information (Table 2) since no Street View imagery is available in the selected geographic location. The reason why this happens is that bridge beginning coordinates provided to OSM by road users does not necessarily correspond to a valid Google Street View location or the road is a rural one on which no image is available.

As can be seen from Table 2, most null images are related to minor road infrastructures and therefore a manual correction of bridge



Fig. 8. Images extracted from Google Street View (the file name corresponds to the bridge ID).

Table 2
Distribution of nulle images by road type.

Road type	Null images
cycleway	1
footway	7
path	11
primary	1
residential	1
road	2
secondary	2
service	9
tertiary	3
track	63
trunk_link	1
unclassified	18
Total	119

coordinates to recover the images would seem to be not so important for the scope of this study, also considering that for some of them no imagery is available at all. In fact, the following sections describe how the selected DL algoritm has been trained and used to detect the guardrail type through the extracted images, only regarding main road infrastructures, which are the most urgent in terms of traffic safety.

2.3. Typological classification of guardrails

According to [5], in case a bridge guardrail is replaced, a new H2, H3, or H4 type barrier must be installed depending on the type of road (motorways, extra-urban roads, and urban roads) and traffic volume (also as a percentage of commercial vehicles with mass higher than 3.5 tons). H2, H3, and H4 barriers have increasing containing capacity and are usually installed on bridge edge curbs through chemical anchors. Fig. 9 compares old bridge barriers (c and d) and a new H3 one (a and b) (e.g., [31]).

As reported in [6], the main difference between old-type bridge barriers and new, code-coforming ones, is that the latter feature the presence of a 3-wave steel railing instead of a weaker 2-wave one mounted on non-conforming barriers. Moreover, the connecting elements installed at the top of the device are more robust to permit a stronger collaboration between consecutive posts, in order to increase the device containing capacity.

Additional types of railings are reinforced concrete New Jersey (NJ) barriers (Fig. 10a), concrete (plain or reinforced) and masonry walls (Fig. 10b) and iron parapets (Fig. 10c). While NJ barriers could be cosidered code conforming due their high crash resistance, both walls and parapets cannot. In fact walls are not tested elements that may



Fig. 10. Additional barrier types: (a) Concrete NJ, (b) masonry or concrete wall and (c) parapet.

guarantee the needed resistance. Moreover, they often feature sharp edges and ends that can be dangerous in case of vehicle impact. On the other hand, iron parapets are too weak to offer some impact resistance. They easily fail even due to low energy impacts and cause the vehicle to fall down the bridge. Therefore detections are assumed as in Table 3, showing that when a non-conforming guardrail is correctly detected, it represents a true positive (TP) detection, assuming positive the cases that need barrier replacement. On the contrary, when a code-conforming guardrail is correctly detected, it is a true negative (TN) in the sense that it is properly identified the absence of any replacement need.

Therefore, when a non-conforming barrier is uncorrectly identified, it is a false positive (FP) while, when a code-conforming barrier is

Table 3
Guardrail classes and detection assumptions.

Barrier description	Abbreviation	Code conforming	Detection assumption	Detection class
Older type metallic guardrail	2-w	no	TP	0
Triple wave H2, H3 or H4 guardrail	3-w	yes	TN	1
Reinforce concrete NJ guardrail	NJ	yes	TN	2
Masonry or RC wall	Wall	no	TP	3
Iron parapet	Parapet	no	TP	4

TP = true positive; TN = true negative

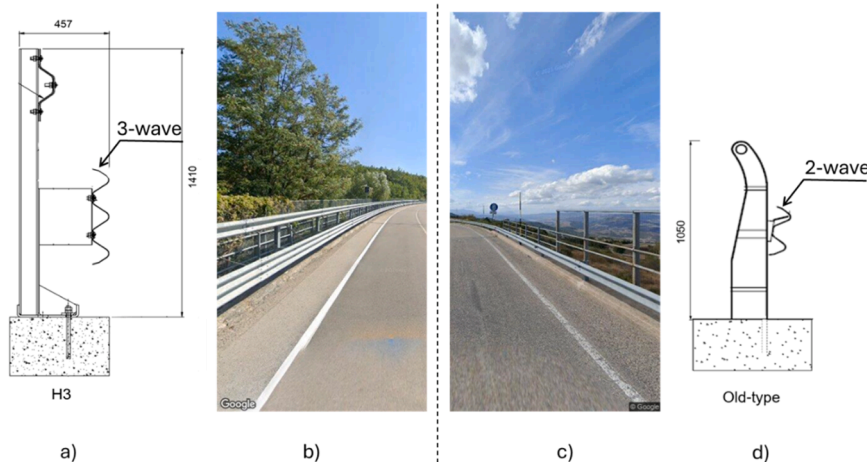


Fig. 9. Grafical comparison between old- and new-type bridge barriers: new type with 3-wave guardrail (a) sketch and (b) picture of an installation. Old-type barrier (c) installation and (d) sketch of the traditional 2-wave guardrail.

wrongly identified, it is a false negative (FN). **Table 3** also shows the detection class that is a more concise class representation during the annotation activities and output elaboration.

2.4. Image labelling and deep learning algorithm for safety barrier detection

Once the images are retrieved from the API, they are processed using the YOLOv8 deep learning algorithm [32]. The YOLO (You Only Look Once) algorithm is a real-time object detection model that frames detection as a single regression problem. Unlike traditional methods that apply region proposal and classification in multiple stages, YOLO processes the entire image in just one step. It subdivides the image into a grid and, for each cell, simultaneously predicts bounding boxes and class probabilities. This unified architecture allows for extremely fast and accurate detection, making it particularly suitable for large-scale applications such as infrastructure monitoring. This algorithm is trained to detect and classify various types of safety barriers, such as guardrails and concrete barriers. The goal is to identify whether the barriers are compliant with current safety standards or if they need to be replaced. It is worth noting that the identification of any damage occurred to the barrier is out of the scope of this study.

By analysing the images, the system must automatically assess the barrier type permitting to identify those that are non-compliant, facilitating the decision-making process for infrastructure maintenance.

This approach allows for efficient, large-scale monitoring of bridge safety in a certain region, reducing the need for manual inspections and enabling the use of automated tools for maintaining road safety standards.

In order to train the YOLOv8 model to specifically recognize guardrails with a relatively low effort, a first annotation task was deployed, selecting 101 images according to **Table 4**. In order to increase the number of images, two types of data augmentation were made: (i) $\pm 15\%$ exposure variation and (ii) $\pm 2.5\%$ blur. These types of augmentations are able to provide the model the ability of making predictions based on varying brightness conditions and also with respect to low quality images having some blurry regions. Therefore, **Table 4** reports the total number of occurrences for each class.

It must be noted that NJ was very rare in the dataset available, therefore training on that class is, as expected, unsuccessful. This prevents the effective prediction of NJ class in the collected images. Some examples of image annotation are reported in **Fig. 11**. As can be noted, annotation was not made through rectangles including the wanted elements. In fact, polygons were used to better highlight the distinctive portions of the barrier. **Fig. 11a** and **b** show polygons including the 2-w and 3-w guardrail tapes since the goal is to detect the main element that characterizes the barrier. There are many types of 2-w and 3-w guardrails. It is not interesting to establish which type of 2-w or 3-w barrier is installed, but if the barrier features a 2-w or a 3-w rail, since this is paramount to know whether it is code conforming or not. Using this approach, also the background disturbance is significantly reduced.

2.5. Integrating open-source tools and deep learning algorithms

This methodology integrates OpenStreetMap (OSM) queries, Google Street View (GSV) image retrieval, and YOLOv8 classification into a

Table 4
Count of annotated images.

Class name	Count	$\pm 15\%$ exposure	± 2.5 pixels blur	Total
2-w	71	71	71	213
3-w	36	36	36	108
NJ	3	3	3	9
Wall	32	32	32	96
Parapet	22	22	22	66

cohesive workflow designed for efficient safety barrier assessments on road bridges. The individual steps detailed previously, were already utilized singularly in previous studies [10,23,27] although their combined use is a novelty and represents a significant advancement of this study.

The integrated dataflow from bridge localization to guardrail type detection was automated by means of Visual Basic for Application (VBA) routines (Macros) integrated in an Excel workbook.

Referring to **Fig. 12**, in Worksheet 1, the process begins with Macro 1, where bridges are extracted from OpenStreetMap (OSM) using a query via the Overpass API. This query identifies features tagged as "bridge=yes" within a specified geographic bounding box, retrieving relevant data in CSV format. Macro 2 processes the extracted data by importing the CSV file into the workbook, assigning unique identifiers to each bridge, and calculating their lengths based on geographic coordinates. The Atan2 function is used to determine heading values, which are then included in Google API requests. These requests fetch Google Street View images for each bridge, which are stored in a specific folder. Macro 3 employs the YOLOv8 model to infer objects within the saved images. The results include labels, bounding boxes, and confidence scores, which are saved in a text format. Macro 4 imports these inference data labels into Worksheet 2, organizing them into columns that feature bridge IDs, class names, and confidence values.

Worksheet 2 focuses on class predictions and uses Macro 5 for analysis. This macro sets up a pivot table to structure the prediction data and applies filters to identify bridges that need guardrail replacement. The filtered data is then exported to Google My Maps to visualize the geographical locations of the affected bridges (**Fig. 3f**).

In Worksheet 3, Macro 6 handles cost computations. It calculates the total bridge lengths requiring guardrail replacement and estimates the associated costs. Finally, bridges are prioritized for replacement based on their road type and length, ensuring an optimized resource allocation. This workflow integrates OSM, Google APIs, and the YOLOv8 model to streamline the evaluation and prioritization of bridge safety interventions.

This streamlined framework represents a key innovation, automating the process and enabling even non-technical users to leverage advanced tools effectively.

3. Analysis of results

The trained YOLOv8 algorithm was applied to a subset of 776 bridges (each one corresponding to a single image) belonging exclusively to the major infrastructures in Basilicata region. The application process is remarkably fast, requiring only a few minutes to process the entire dataset.

The predictions were evaluated using a test set of 194 images, corresponding to 25 % of all the images considered. For each image, the algorithm provided one or more object classes along with their respective confidence scores. The final class assigned to each image was the one with the highest confidence. The comparison with the annotations of the test set images permitted to obtain the real guardrail type distribution over the test set, as reported in **Fig. 13**.

As expected for major road infrastructures, the presence of Wall and Parapets guardrails is low, being 3.1 % and 1.0 %, respectively. While the majority of barrier are code conforming 3-w guardrail, a significant share (46.4 %) is represented by 2-w outdated barriers. Some examples of guardrail detections are shown in **Fig. 14**.

In order to evaluate the detection capacity of the trained algorithm, one must consider that the Intersection over Union (IoU) metric is commonly used to assess the degree of overlap between predicted bounding boxes and the ground truth bounding boxes. IoU is calculated as the ratio of the intersection area to the union area of the two boxes, and it is critical for determining whether a predicted box is accurate. However, in this specific problem, the focus is just on classification rather than precise localization of objects. The objective is to identify the

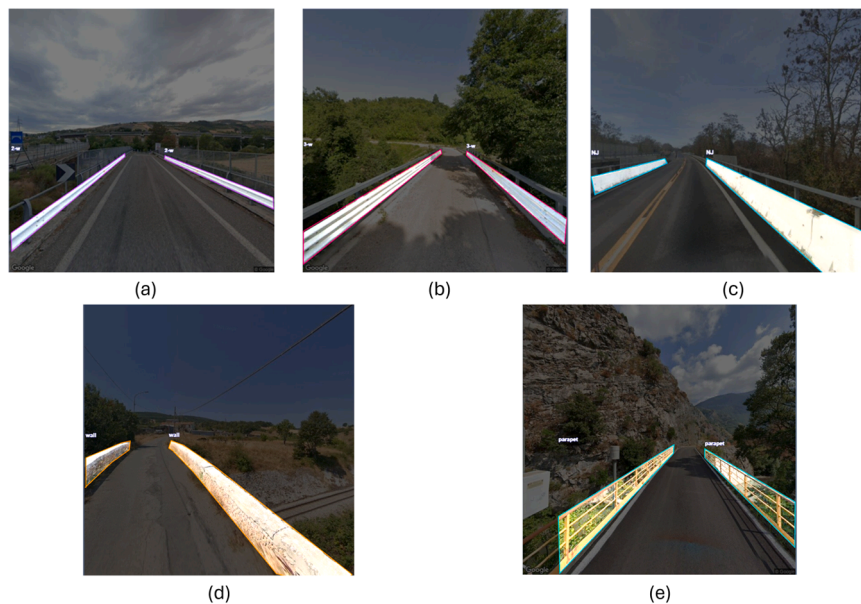


Fig. 11. Examples of image annotations: (a) 2-w, (b) 3-w, (c) NJ, (d) Wall, (e) Parapet.

WorkSheet 1 – Bridge database construction and GSV image extraction

Macro 1 – Extracting bridges from OSM

```
[out:json][timeout:25];
(
  way["bridge"="yes"];(bounding_box);
  relation["bridge"="yes"];(bounding_box);
);
out body;
>;
out skel qt;
```

Macro 2

- 2.1 Importing data from CSV generated and downloaded from OSM;
- 2.2 Assigning unique bridge IDs
- 2.3 Calculating bridge lengths from Lat. & Lon.
- 2.3 Calculation of Atan2 (as heading values in Google API request)
- 2.4 Generation of Google API requests for each bridge

2.5 Execution Google API requests for each bridge, saving GSV images into a specified folder

Macro 3 – Inferring extracted images with YOLOv8

```
yolo task=detect ^
mode=predict ^
model=C:/MyYoloTrainedModelPath/runs/ ^
detect/train6/weights/best.pt ^
source=C:/MySavedGSVimages ^
save=True ^
save_txt=True ^
save_conf=True
```

Macro 4 - Importing data labels deriving from inference into Worksheet 2 featuring 11 columns (IDs, 5 classes names, 5 confidence values);

WorkSheet 2 – Class predictions

Macro 5 –

- 5.1 Setting up pivot table for prediction data analysis
- 5.2 Filtering bridges needing guardrail replacement
- 5.3 Exporting data to Google Mymaps for bridge geographical visualization

WorkSheet 3 – Cost computation

Macro 6 –

- 6.1 Calculating bridge length needing guardrail replacement
- 6.2 Calculating cost for bridge needing guardrail replacement
- 6.3 Prioritization based on Road Type and Length

Fig. 12. Workflow of the integrated bridge guardrail assessment procedure.

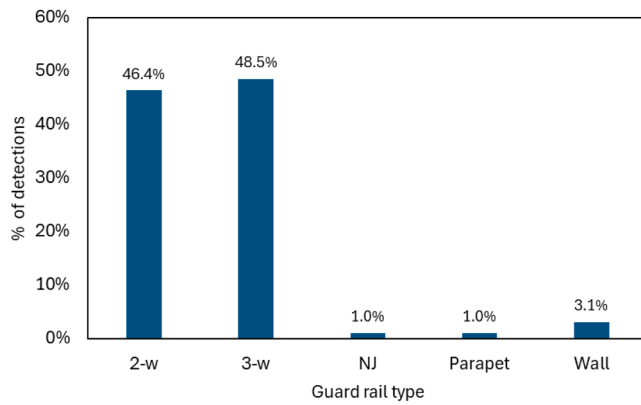


Fig. 13. Distribution of guardrail types over the test set.

correct class associated with each image, regardless of the exact position of the bounding boxes. Therefore, IoU is not relevant in this context, as the evaluation does not depend on spatial accuracy but rather on the model's ability to assign the correct class to each instance.

Therefore, the used metrics were Accuracy, Recall (R), Precision (P), and F1-Score defined as follows:

$$\text{Accuracy} = \frac{TP + TN}{TP + FP + TN + FN} \quad (1)$$

$$R = \frac{TP}{TP + FN} \quad (2)$$

$$P = \frac{TP}{TP + FP} \quad (3)$$

$$F1.\text{score} = 2 \cdot \frac{P \cdot R}{P + R} \quad (4)$$

Where:

- TP: True Positives
- FP: False Positives
- TN: True Negatives
- FN: False Negatives

In this application, a False Negative represents a failure to recognize a non-compliant barrier, which could lead to lack of action on a possibly vulnerable structure. Such oversights could have serious safety implications, as these barriers may not meet the necessary standards for protecting road users.

While Precision measures how many of the predicted non-compliant barriers are actually correct, it is less critical in this case because False Positives (FP) simply result in additional checks on barriers that are ultimately compliant, which is less dangerous than missing a non-compliant one.

Therefore, prioritizing Recall aligns with the safety-first approach required in this domain, ensuring a thorough identification of non-compliant barriers to mitigate potential risks.

To better understand the performance of the algorithm, the test set was divided based on confidence thresholds. Table 5 summarizes Recall and False Positive Rate (FPR) across different thresholds:

Summarizing the previous metrics, the following results are obtained:

- Accuracy: 0.912
- Recall (R): 0.928
- Precision (P): 0.900



Fig. 14. Examples of detections of (a) 3-w, (b) 2-w, (c) Parapet and (d) Walls.

Table 5
Detection results over the test set.

Confidence	TP	FP	TN	FN	Recall	FPR
0.4	7	4	4	1	0.875	0.500
0.5	15	5	6	2	0.882	0.455
0.6	24	5	12	6	0.800	0.294
0.7	35	7	18	6	0.854	0.280
0.8	49	9	24	6	0.891	0.273
0.9	63	10	42	7	0.900	0.192
1	90	10	87	7	0.928	0.103

- F1-Score: 0.914

These values indicate that the algorithm performs well in detecting relevant objects while maintaining a high level of Precision. Accuracy measures the proportion of correct predictions made out of all predictions and provides an indication of how often the model is correct in its classifications. The high value achieved demonstrates the model's effectiveness. The high F1-Score highlights a good balance between Recall and Precision.

Data in Table 5 shows that as the confidence threshold increases Recall improves, reaching a maximum of 0.93 at a confidence of 1.0. This indicates that higher confidence thresholds lead to fewer False Negatives, as expected; FPR decreases significantly, reaching 0.10 at the highest confidence threshold. This highlights the algorithm's ability to reduce False Positives at higher confidence levels.

The relationship between Recall (and FPR) and confidence thresholds is depicted in the graph of Fig. 15, demonstrating the algorithm's performance at varying levels of confidence. Moreover, the Recall local minimum value at Confidence 0.6 depends on the sharp increase of FN as the Confidence passes from 0.5 to 0.6.

This graph confirms the expected trend: as confidence increases, the TPR improves, and the FPR drops. This behaviour aligns with the goal of optimizing both Recall and Precision at higher confidence levels. The results further validate the robustness of the trained YOLOv8 algorithm for automatic classification tasks on major infrastructure datasets.

In order to understand the model's detection capacity about single classes, the normalized confusion matrix is depicted in Fig. 16. This latter reveals the performance of the classification model across five safety barrier classes: 2-w, 3-w, NJ, Parapet, and Wall. The results show that the model provides high classification accuracy for the 2-w and 3-w classes, correctly identifying 92 % of the instances. However, there is some overlap between these two classes, with 7 % of 2-w barriers misclassified as 3-w and vice versa. In fact, these classes share similar features, related to the 2-w steel tape that in some lighting condition or in

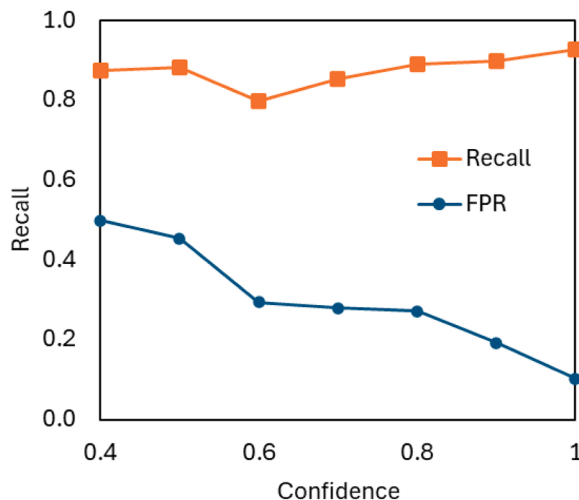


Fig. 15. Recall and FPR as a function of confidence.

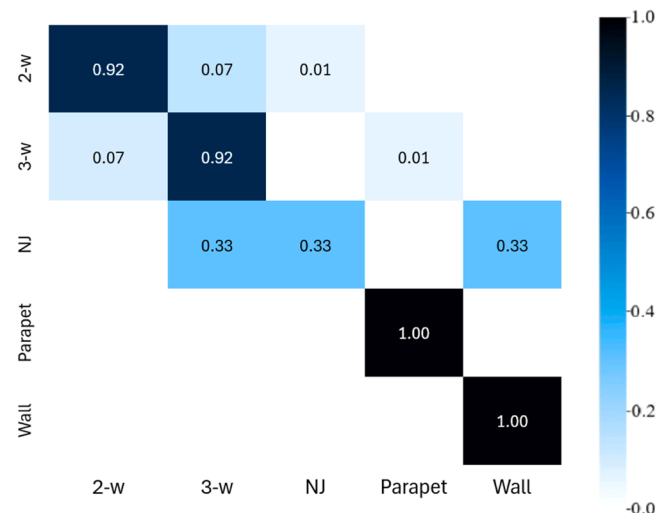


Fig. 16. Results of YOLOv8 in terms of normalized confusion matrix.

presence of vegetation may potentially be confused with 3-w and vice versa. For the NJ class, the performance is remarkably lower, with an accuracy of only 33 %. As expected, NJ misclassifications are with Wall classes but also regarding 3-w, indicating that the distinguishing features of NJ barriers are not well captured by the model. However, this does not impact so much the overall procedure since very fewer NJ cases are present in the database.

On the contrary, the model performs perfectly for the Parapet and Wall classes, achieving 100 % accuracy. These results indicate that these classes possess evident features the model is able to learn effectively, leading to no observed misclassifications.

Given the mentioned misclassification problems, future improvements could include enlarging the training set, applying more diverse augmentation, and incorporating additional features like texture or background context. Rare classes like NJ barriers are more difficult to detect due to the small sample size, and this will also be acknowledged with possible solutions such as targeted data collection or synthetic data generation.

4. Cost analysis and prioritization

Once the trained deep learning model's ability has been checked through the previously mentioned metrics, the result in terms of guardrail classification can be assumed reliable and helpful in a regional cost prediction about the replacement of safety barrier along the selected major road infrastructures. The previous analysis show that Wall- and Parapet-type barriers are negligible over these infrastructures, and therefore in the following cost predictions, only 2-w guardrails will be considered.

It must be noted that, the cost prediction is based on [6], in which parametric costs were reported based on the price list of ANAS [33], which is the major road management body in Italy. The technical solutions are also based on the design manual issued by the same agency [34] and foresee the guardrail replacement along with the strengthening of the cantilever part of the slab [6]. As can be seen from Fig. 17, the unit length cost varies between 744 €/m and 1042 €/m, according to the width of the bridge slab to be strengthened. It is also assumed that in place of the 2-w guardrail a H4 (the highest containment class) code-conforming guardrail is installed.

Adopting a mean cost value equal to $C = 893$ €/m and considering that each bridge equipped with non-compliant guardrails has two sides needing replacement, the total intervention cost can be easily computed.

As presented in Table 6, the total cost of intervention to replace 2-w barriers overcomes 67 million Euro. Considering that the used price list

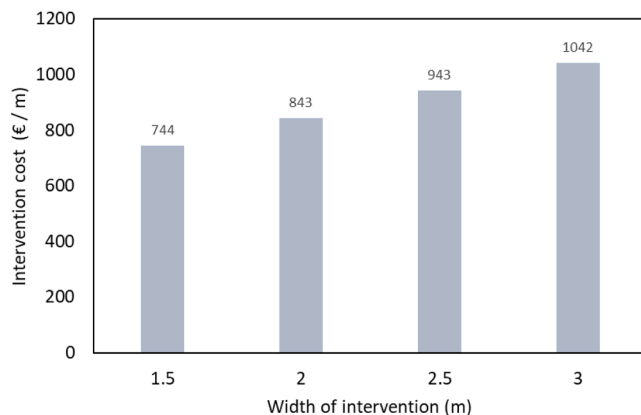


Fig. 17. Guardrail replacement cost (Adapted from [6]).

Table 6
Summary of cost calculations.

Data description	Amount	Units
Number of bridges on major infrastructures	776	–
Number of bridges equipped with 3-w guardrails	454	–
Number of bridges equipped Parapets, Walls and NJ	29	–
Number of bridges equipped with 2-w guardrails	293	–
Length of bridges equipped with 2-w guardrails	37.54	km
Length of guardrails replacement	75.09	km
Mean cost of intervention C	893	€/m
Total cost of intervention	67.05	M€

dates to year 2022, the actualized cost in 2025 would correspond to 71.5 million Euro.

Besides the cost prediction to make all bridge barriers code-compliant, a prioritization scheme is needed to obtain an optimal resource allocation. The scheme used in this study is based on the fact that major road infrastructures are more prone to accidents due to higher speed, larger traffic volume and higher percentage of commercial vehicles, which are more likely to cause the guardrail collapse in case of an impact [6]. Therefore, higher priority is given to bridges on these road infrastructures according to the order of Table 1. When dealing with bridges on the same road type, the priority is assigned based on length values, in the sense that longer bridges must have a higher priority. In fact, the probability that an accident happens increases with the bridge length. This approach, although reasonable, lacks data on real traffic volumes. In fact, it is assumed that infrastructures within the same road type have equal traffic volumes, and this is generally false, although in some cases differences may be negligible. The resulting list of priorities is not reported due to discretion, even though the bridges needing barrier replacement are visually located in Fig. 3(f).

5. Discussion

The proposed methodology for automating the classification of safety barriers on bridges represents a significant advancement in the management of critical infrastructure. This approach, utilizing open-source data such as OpenStreetMap (OSM) and the Google Street View API alongside deep learning algorithms like YOLOv8, addresses multiple challenges faced by local authorities responsible for road safety in an integrated manner. Strengths and limitations of the proposed methodology are summarized in the flowchart of Fig. 18.

One of the key advantages of the methodology is its use of publicly available data and scalable computational tools. The use of OSM for extracting bridge coordinates and Google Street View for image retrieval eliminates the need for expensive and time-consuming data acquisition technologies such as laser scanning or drone surveys. This makes the approach highly cost-effective and accessible to local road authorities

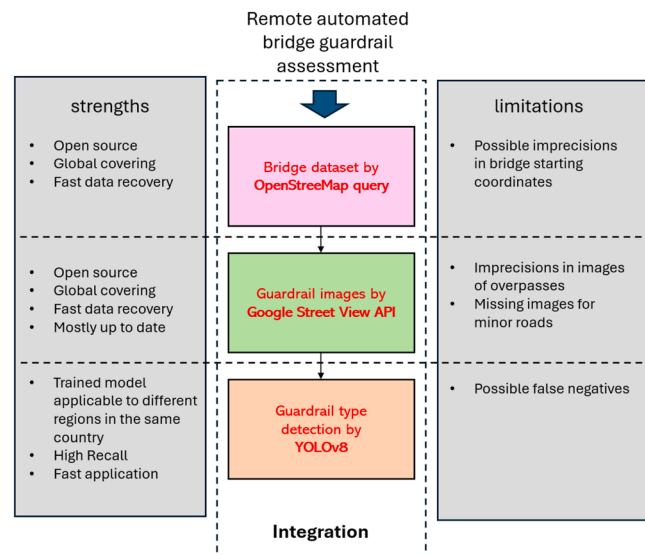


Fig. 18. Strengths and limitations of the proposed methodology.

with limited budgets and technical expertise. The capability to process large datasets in just a few minutes further evidences its practical value, allowing for rapid assessments of large road networks. However, for some bridges, the starting coordinates could be imprecise and this may impact on the Street View images that may refer to a guardrail on a road portion before the bridge.

The use of Google Street view API allows to have open access to valuable images, practically worldwide, and big set of image can be retrieved rapidly. In most cases these images are up to date and present the actual condition of bridge barriers.

On the other hand, when the bridge at hand is an overpass, sometimes the provided image is related to the road below, that is not useful for the scope. Moreover, as seen before, bridges on minor roads could be not covered by this service.

To overcome these issues, when GSV images are not available, the only solution is to carry out a manual inspection to collect the necessary data. Conversely, the issue of inaccurate bridge coordinates can be identified by examining the initial GSV image: if the heading angle is incorrect, the guardrails may not be visible. Bridges affected by this problem can be easily and automatically identified, as the YOLO algorithm produces no detections—an unlikely outcome, since every bridge should feature either a compliant or non-compliant barrier. This specific issue can be resolved by manually retrieving the correct image from GSV using a manually adjusted heading angle. Although these steps require some manual intervention, addressing such issues would significantly enhance the overall applicability of the proposed methodology.

Finally, YOLO object detection algorithm is known for his speed of elaboration, which does not even need particularly powerful computers. The trained model has a general validity for a given country. For example in Italy guardrail type are quite uniform alongside the different regions, and the resulting model can be used also for regions different from that one the model is trained on. While the whole method is technically applicable worldwide (as OSM and Google Street View are available in many regions), its effectiveness in countries other than Italy depends on the need to train the YOLO algorithm with respect to local barrier types, in order to be adapted for its intended use.

Overall, the major strength of the methodology is represented by the possibility to easily integrate different steps into a simple software tool and to operate remotely, greatly reducing inspections, personnel and expensive devices requirements.

The application of the methodology to a subset of 776 bridges in Basilicata region highlights its practical utility. By focusing on major

road infrastructures, where traffic volumes and safety risks are highest, the study effectively identifies the structures needing intervention. The analysis of a test set comprising 194 images demonstrated the robustness of the YOLOv8 algorithm, which achieved Accuracy of 0.912, Recall of 0.928, Precision equal to 0.900 and F1-Score 0.914. These metrics underline the algorithm's ability to accurately classify guardrails, particularly in detecting non-compliant ones.

The results also show the importance of focusing on Recall in this context. A high Recall values ensures that the majority of non-compliant guardrails are identified, thus minimizing the risk of leaving unsafe structures undetected. False negatives, in this context, could lead to serious safety risks and potentially catastrophic consequences. Event though Precision is less critical, the high value achieved in the study evidences that the algorithm results a low rate of false positives, reducing unnecessary inspections or interventions. However, a certain level of false positives is acceptable in the context of this study, as the primary objective is not to achieve perfect classification on every single bridge, but rather to provide a reliable estimate of the barriers that may require replacement for prioritisation purposes.

The analysis of results based on confidence thresholds provides deeper insights into the algorithm's performance. As the confidence threshold increases, the False Positive Rate (FPR) decreases to 0.10. This trend is in line with the expectation that higher confidence thresholds yield more reliable classifications, reducing the probability of false negatives.

The cost analysis presented in the study provides a valuable perspective on the economic implications of replacing non-compliant barriers. The estimated cost of €71.5 million for replacing 2-wave barriers with code-compliant 3-wave barriers underscores the financial burden of ensuring passive road safety on bridges. The proposed prioritization scheme puts in evidence the importance of Road Type data and bridge length although needing accurate data on traffic volumes. Overall, the cost computation highlights the necessity of accurate and efficient classification methods to prioritize interventions and allocate resources effectively.

Referring to the 776 bridges inferred by the procedure, acting thorough traditional bridge visual inspections (with lane closures) would take 194 days (4 bridges per day, see [Section 2](#)) and 10 days using high-resolution cameras mounted on a vehicle with subsequent data analysis. Using the proposed methodology only requires few hours since it could be based on the already trained model (the one proposed here). Furthermore, the proposed methodology provides fully connection of visual (GSV) and non visual data (bridge data) with geographic locations, permitting the full exploitation of open source tools. The time and cost savings obtained through this approach are not quantified here but represent an important added value for a timely prioritization of maintenance interventions.

6. Conclusions

The proposed methodology provides an innovative approach to infrastructure management and demonstrates the feasibility of large-scale assessments of bridge safety barriers along with the following main strengths:

- It minimizes the manual effort allowing to operate with a fully automated and remote approach, which significantly reduces the time and cost associated with manual inspections, allowing for faster and more comprehensive assessments of road infrastructure.
- The proposed framework can be applied to the entire Italian country and also exported to different countries with the only need to train the YOLO model based on local types of guardrails, considering that OSM and Street View data are available almost globally.
- The integrated data retrieving and analysis approach does not require sophisticated software tools nor powerful computer infrastructure, being based on simple VBA routines concatenated each other.

The methodology applied to 776 bridges in Basilicata region showed its practical utility in detecting and classifying safety barriers. The results from a test on 194 images revealed a high Recall equal to 0.928, ensuring that the majority of unsafe barriers are identified, addressing a critical priority in road safety.

Therefore, the methodology enables critical entities (road management bodies) to prioritize interventions on high-risk structures, optimizing resource allocation and increasing the asset management sustainability.

A possible future development could be represented by the possibility to assess eventual guardrail physical damage or deterioration, which are critical factors in assessing barrier safety, even for code conforming ones. Incorporating damage detection capabilities into the framework could further enhance its utility. Such a damage detection YOLO model would be separate from the classification model, and could be specific for each barrier type. This would require each damage detection model to be applied after the inference, based on the classification result.

CRediT authorship contribution statement

Giuseppe Santarsiero: Writing – review & editing, Writing – original draft, Visualization, Validation, Supervision, Software, Resources, Project administration, Methodology, Investigation, Funding acquisition, Formal analysis, Data curation, Conceptualization.

Declaration of competing interest

I have the authors declare that they have no known competing financial interests or personal relationships that could have appeared to influence the work reported in this paper.

Data availability

Data will be made available on request.

References

- [1] A.C.P. Martins, J.M. Franco de Carvalho, M.C.S. Alvarenga, D.S.D Oliveira, K.M. L. César Jr, J.C.L. Ribeiro, R.C. Verly, Detecting, monitoring and modeling damage within the decision-making process in the context of managing bridges: a review, *Struct. Infraract. Eng.* (2024) 1–23, <https://doi.org/10.1080/15732479.2024.2331103>.
- [2] G. Miluccio, D. Losanno, F. Parisi, E. Cosenza, Fragility analysis of existing prestressed concrete bridges under traffic loads according to new Italian guidelines, *Struct. Concr.* 24 (1) (2023) 1053–1069, <https://doi.org/10.1002/suco.202200158>.
- [3] L. Thanh, Y. Itoh, Performance of curved steel bridge railings subjected to truck collisions, *Eng. Struct.* 54 (2013) 34–46.
- [4] S. Galano, D. Losanno, F. Parisi, Numerical simulation of post-tensioned concrete girders with defective grouting including local stress-strain tendons response, *Struct. Concr.* 25 (6) (2024) 4515–4536, <https://doi.org/10.1002/suco.202400416>.
- [5] MIT (Ministry of Infrastructure and Transportation) DM 21/06/2004 n. 2367; Aggiornamento dei istruzioni tecniche per la progettazione, l'omologazione e l'impiego delle barriere stradali di sicurezza e le prescrizioni tecniche per le prove delle barriere di sicurezza stradale (G.U. 06/08/2004, n. 182).
- [6] G. Santarsiero, Retrofitting of bridge slabs for safety railing refurbishment in Italy: a state-of-the-art review, *Appl. Sci.* 13 (21) (2023) 12051, <https://doi.org/10.3390/app132112051>.
- [7] J. Rymsza, Causes of the collapse of the Polcevera Viaduct in Genoa, Italy, *Appl. Sci.* 11 (17) (2020) 8098, <https://doi.org/10.3390/app11178098>.
- [8] MIT (Ministry of Infrastructure and Transportation) - High Council of Public Works (CSLP), Guidelines on Risk Classification and Management, Safety Assessment and Monitoring of Existing Bridges, Ministry of Infrastructure, Rome, Italy, 2020.
- [9] MIT (Ministry of Infrastructure and Transportation) - Decreto Ministeriale Numero 204 del 1 luglio 2022. Linee Guida per la classificazione e gestione del rischio, la valutazione della sicurezza ed il monitoraggio dei ponti esistenti. Rome, Italy, 2022.
- [10] G. Santarsiero, A. Masi, V. Picciano, A. Digrisolo, The Italian guidelines on risk classification and management of bridges: applications and remarks on large scale risk assessments, *Infrastructures* 6 (2021) 111. [\(Basel\)](#).
- [11] F. Brighenti, V.F. Caspani, G. Costa, P.F. Giordano, M.P. Limongelli, D. Zonta, Bridge management systems: a review on current practice in a digitizing world,

Eng. Struct. 321 (2024) 118971, <https://doi.org/10.1016/j.engstruct.2024.118971>.

[12] S. Sivaraos, P.K. Prasath, S. Ramesh, K. Kadrigama, M.S. Salleh, M.A.A. Ali, S. Maidin, T.K. David, Rooted guardrail post design - an improvement towards reducing run-off-road catastrophic accidents, *AIP Conf. Proc.* 2643 (2023) 050026.

[13] A. Nemati, M. Haas, D. Torick, et al., Lifetime cost analysis of concrete barriers and steel guardrails, *Sci. Rep.* 14 (2024) 15699, <https://doi.org/10.1038/s41598-024-66090-1>.

[14] Casas J.R. (2024) Sustainability and digitalization in bridge management: how far we are? *Bridge maintenance, safety, management, digitalization and sustainability* – Jensen, Frangopol & Schmid (eds) © 2024 The Author(s), ISBN 978-1-032-77040-6 Open Access: www.taylorfrancis.com, CC BY-NC-ND 4.0 license.

[15] W. Zhang, N. Wang, Bridge network maintenance prioritization under budget constraint, *Struct. Saf.* 67 (2017) 96–104, <https://doi.org/10.1016/j.strusafe.2017.05.001>.

[16] W.S. Qureshi, D. Power, I. Ullah, B. Mulry, K. Feighan, S. McKeever, D. O'Sullivan, Deep learning framework for intelligent pavement condition rating: a direct classification approach for regional and local roads, *Autom. Constr.* 153 (2023) 104945, <https://doi.org/10.1016/j.autcon.2023.104945>.

[17] A. Broggi, P. Cerri, F. Oleari, M. Paterlini, Guard rail detection using radar and vision data fusion for vehicle detection algorithm improvement and speed-up, in: *Proceedings of the IEEE Intelligent Transportation Systems, Vienna, Austria, 2005*, pp. 552–556, <https://doi.org/10.1109/ITSC.2005.1520162>, 2005.

[18] A. Wimmer, T. Weiss, F. Flögel, K. Dietmayer, Automatic detection and classification of safety barriers in road construction sites using a laser scanner, in: *Proceedings of the IEEE Intelligent Vehicles Symposium, Xi'an, China, 2009*, pp. 578–583, <https://doi.org/10.1109/IVS.2009.5164342>.

[19] J. Gao, Y. Chen, J.M. Junior, C. Wang, J. Li, Rapid extraction of urban road guardrails from mobile LiDAR point clouds, *IEEE Trans. Intel. Transp. Syst.* 23 (2) (2022) 1572–1577, <https://doi.org/10.1109/TITS.2020.3025067>, Feb.

[20] Q. Zhou, Z. Liu, Z. Huang, Mapping road surface type of Kenya using OpenStreetMap and high-resolution Google satellite imagery, *Sci. Data* 11 (2024) 331, <https://doi.org/10.1038/s41597-024-03158-7>.

[21] M. Haklay, P. Weber, OpenStreetMap: user-generated mapping, *Future Internet* 2 (1) (2020) 282–303.

[22] J.E. Vargas-Munoz, S. Srivastava, D. Tuia, A.X. Falcão, OpenStreetMap: challenges and opportunities in machine learning and remote sensing, *IEEE Geosci. Remote Sens. Mag.* 9 (1) (2021) 184–199, <https://doi.org/10.1109/MGRS.2020.2994107>.

[23] L. Rita, M. Peliteiro, T. Bostan, T. Tamagusko, A. Ferreira, Using deep learning and Google street view imagery to assess and improve cyclist safety in London, *Sustainability* 15 (13) (2022) 10270, <https://doi.org/10.3390/su151310270>.

[24] Google Inc. 2024. Google maps platform, overview on API roads <https://developers.google.com/maps/documentation/roads/overview?hl=it>.

[25] Redmon, J., & Farhadi, A. (2018). YOLOv3: an incremental improvement. arXiv preprint arXiv:1804.02767.

[26] D. Liang, S. Zhang, H. Huang, L. Zhang, Y. Hu, Deep learning-based detection and condition classification of bridge elastomeric bearings, *Autom. Constr.* 166 (2024) 105680, <https://doi.org/10.1016/j.autcon.2024.105680>.

[27] Alhasoun, M. González, Streetify: using street view imagery and deep learning for urban streets development, in: *Proceedings of the IEEE International Conference on Big Data (Big Data), Los Angeles, CA, USA, 2019*, pp. 2001–2006, <https://doi.org/10.1109/BigData47090.2019.9006384>.

[28] W. Wang, C. Su, Deep learning-based detection and condition classification of bridge steel bearings, *Autom. Constr.* 156 (2023) 105085, <https://doi.org/10.1016/j.autcon.2023.105085>.

[29] OSM – Openstreetmap, 2024 <https://wiki.openstreetmap.org/wiki/Tags> (Accessed on 24 September 2024).

[30] Microsoft (2024). Office VBA Reference <https://learn.microsoft.com/en-us/office/vba/api/overview/>.

[31] Buildtech, M. Technical specification of road railings. 2023. Available online: <https://www.marcegagliabuildtech.it/barriere-sicurezza/> (accessed on 28 October 2024).

[32] C. Zong, K. Meng, J. Sun, Q. Zhou, Real time object recognition based on YOLO model, in: *Proceedings of the 3rd International Conference on Electronic Information Engineering and Computer Science (EIECS), Changchun, China, 2023*, pp. 197–202, <https://doi.org/10.1109/EIECS59936.2023.10435392>.

[33] ANAS, Price List/Prezzo (2022). New construction and scheduled maintenance. Available online: <https://www.stradeanas.it/elenco-prezzi> (accessed on 26 September 2024). (In Italian).

[34] ANAS, Quaderni tecnici per la salvaguardia delle infrastrutture, *Quad. Tec.* 17 (2019) 76.